X-ray Diffraction and Gradient-Assisted 2D $^{1}H-^{119}Sn$ HMQC NMR Studies on the Structure of Condensation Complexes of Salicylaldoxime and Dimethyltin(IV) Oxide

Rudolph Willem,*[,†,‡] Abdeslam Bouhdid,[‡] François Kayser,[†,‡] Ann Delmotte,[‡] Marcel Gielen,[‡] José C. Martins,[†] Monique Biesemans,[†,‡] Bernard Mahieu,[§] and Edward R. T. Tiekink[||]

High Resolution NMR Centre (HNMR) and Department of General and Organic Chemistry of the Faculty of Applied Sciences (AOSC), Free University of Brussels (VUB), Pleinlaan 2, B-1050 Brussels, Belgium, INAN, Université Catholique de Louvain (UCL), Chemin du Cyclotron 2, B-1348 Louvain-la-Neuve, Belgium, and Department of Chemistry, The University of Adelaide, Adelaide, Australia

Received December 1, 1995[⊗]

Reaction of dimethyltin(IV) oxide with salicylaldoxime in the molar ratio 3:2 or 1:1 in refluxing toluene/ethanol (4/1) affords reaction mixtures which, upon crystallization from alcohols TOH (T = Me, Et, *n*-Pr, *i*-Pr), generate compounds with three dimethyltin and two salicylaldoximate moieties. These compounds obey the formula [$(Me_2Sn)(Me_2SnO)(Me_2SnOT)$(HONZO)(ONZO)], where HONZOH represents salicylaldoxime, *o*-HON=CHC_6H_4OH. X-ray diffraction analysis of the compounds at room temperature (T = Me, compound **3**; T = Et, **4**; T = *n*-Pr, **5**; T = *i*-Pr, **6**) reveals that all structures contain one seven-coordinate tin atom bound to two nitrogen and three oxygen atoms in the equatorial plane of a pentagonal bipyramid, the two methyl groups being in apical positions. The two other tin atoms are five-coordinate with a trigonal-bipyramidal geometry having the two methyl groups and a common oxygen atom in the equatorial positions and, in apical positions, two further oxygen atoms, of which the trifurcated alkoxy oxygen atom bridges these tin atoms. Reaction of dimethyltin(IV) oxide with salicylaldoxime in the molar ratio 1:1 in refluxing benzene generates, after solvent evaporation, compound **2b**, obeying the formula [$(Me_2Sn)_2(Me_2SnO)$-(HONZO)(ONZO)(HOZNO)]. The solution-state structures of the alkoxy-bridged compounds **3**−**6**, investigated by gradient-assisted 2D $^{1}H-^{119}Sn$ HMQC as well as $^{1}H-^{13}C$ HMQC and HMBC NMR spectroscopy, are the same as those in the solid state. The bonding mode of the third ligand (i.e. HOZNO) of compound **2b** has been elucidated.

Introduction

Unlike diorganotin(IV) carboxylates,[1] the structures of condensation compounds obtained from salicylaldoxime, *o*-HON=CHC_6H_4OH, and di-*n*-butyltin(IV) oxide, Bu_2SnO, are complex and unsymmetric.[2] Condensing salicylaldoxime and di-*n*-butyltin(IV) oxide in molar ratios of 1:1, 2:3, and 1:2 generates after crystallization from various solvents, including ethanol, compound **1a** (Figure 1).[2]

Compound **1a** has the formula [$(Bu_2Sn)(Bu_2SnO)(Bu_2$-SnOH)(HONZO)(ONZO)], where HONZO represents the *o*-HON=CHC_6H_4O− phenolate residue derived from salicylaldoxime, HONZOH, and ONZO represents the *o*-(−ON=CHC_6H_4O−) bidentate ligand. Its structure consists of three di-*n*-butyltin and two salicylaldoximate moieties involved in an unsymmetric network of tin−oxygen and tin−nitrogen bonds with one seven-coordinate and two five-coordinate tin atoms.

Compound **1a** in solution exists as a mixture of several transient species,[2] the structures of which were elucidated by 2D $^{1}H-^{119}Sn$ HMQC spectroscopy.[3]

Condensation in the molar ratio 1:1 of salicylaldoxime and di-*n*-butyltin(IV) oxide followed by rapid evaporation of the solvent resulted in an oily impure compound, **1b**. Attempts to crystallize **1b** either failed or provided crystals of **1a**.[2] Compound **1b**, which was previously assigned the formula[2] [$(Bu_2Sn)_2(Bu_2SnO)(HONZO)_2$-(ONZO)], has roughly the structure of **1a** with the bridging hydroxy group being substituted by a third salicylaldoximate ligand (Figure 1).

During the course of an investigation on the reactivity of such complexes, we attempted to synthesize *mutatis mutandis* their dimethyltin analogs. Unexpectedly, attempts to isolate the dimethyltin analog, **2a**, of compound **1a** as a crystalline compound failed. Crystalline compounds amenable to X-ray analysis could be isolated only when crystallizations of the reaction mixtures were conducted from low molar mass alcohols.

* To whom correspondence should be addressed. E-mail: rwillem@vnet3.vub.ac.be.
† HNMR, Free University of Brussels.
‡ AOSC, Free University of Brussels.
§ Université Catholique de Louvain.
|| The University of Adelaide.
⊗ Abstract published in *Advance ACS Abstracts,* March 1, 1996.

(1) Tiekink, E. R. T. *Appl. Organomet. Chem.* **1991**, *5*, 1. Tiekink, E. R. T. *Trends Organomet. Chem.* **1994**, *1*, 71.

(2) (a) Kayser, F.; Biesemans, M.; Bouâlam, M.; Tiekink, E. R. T.; El Khloufi, A.; Meunier-Piret, J.; Bouhdid, A.; Jurkschat, K.; Gielen, M.; Willem, R. *Organometallics* **1994**, *13*, 1098. (b) Kayser, F.; Biesemans, M.; Bouâlam, M.; Tiekink, E. R. T.; El Khloufi, A.; Meunier-Piret, J.; Bouhdid, A.; Jurkschat, K.; Gielen, M.; Willem, R. *Organometallics* **1994**, *13*, 4126.

(3) (a) Bax, A.; Summers, M. F. *J. Am. Chem. Soc.* **1986**, *108*, 2093. (b) Bax, A.; Summers, M. F. *J. Magn. Reson.* **1986**, *67*, 565. (c) Kayser, F.; Biesemans, M.; Gielen, M.; Willem, R. *J. Magn. Reson.* **1993**, *A102*, 249. (d) Bax, A.; Griffey, R. H.; Hawkins, B. L. *J. Magn. Reson.* **1983**, *55*, 301.

0276-7333/96/2315-1920$12.00/0

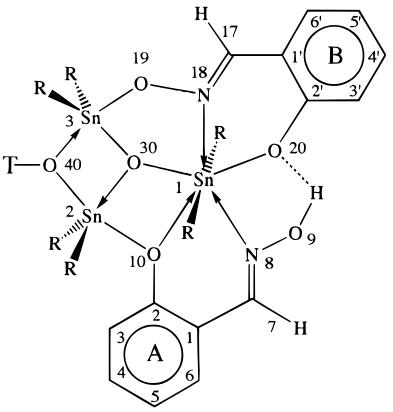

	T	R
1a	H	n-Bu
1b	HOZN	n-Bu
2a	H	Me
2b	HOZN	Me
3	Me	Me
4	Et	Me
5	n-Pr	Me
6	i-Pr	Me

Figure 1. General structures, with atom labeling, of compounds from several reaction mixtures of the condensation reaction between di-*n*-butyl- or dimethyltin(IV) oxide and salicylaldoxime.[2] HOZN stands for *o*-$HOC_6H_4CH{=}N-$.

New alkoxy-bridged structures have been obtained. This report presents the results of structural investigations in the solid state by X-ray diffraction and in solution by 1D and 2D NMR, mainly gradient-assisted[4] $^1H-^{119}Sn$ HMQC and $^1H-^{13}C$ HMBC spectroscopy,[2,3] on these new compounds. The solution structure of **2b**, the dimethyltin analog of **1b**, is elucidated, and the previous structure[2] of **1b** reconsidered.

Results and Discussion

Synthesis. Condensation of dimethyltin(IV) oxide and salicylaldoxime in the molar ratio 1:1 or 2:3 in refluxing toluene/ethanol (4/1 v/v) with elimination of water gives rise, after solvent evaporation, to an oily reaction mixture. Unlike the analogous reaction mixture from di-*n*-butyltin(IV) oxide,[2] crystallizations from cyclohexane and acetonitrile failed to generate the desired crystals of compound **2a** (Figure 1), the dimethyltin analog of the di-*n*-butyltin compound **1a**. However, when the alcohol TOH is used as a crystallization solvent (T = Me, Et, *n*-Pr, *i*-Pr), four new compounds (**3**−**6**; Figure 1) are generated; all four of them provided crystals suitable for X-ray diffraction analysis.

In analogy with compound **1a**, the new compounds can be represented by the general formula [(Me_2Sn)-$(Me_2SnO)(Me_2SnOT)$(HONZO)(ONZO)], with T = Me (**3**), Et (**4**), *n*-Pr (**5**), and *i*-Pr (**6**). The new compounds

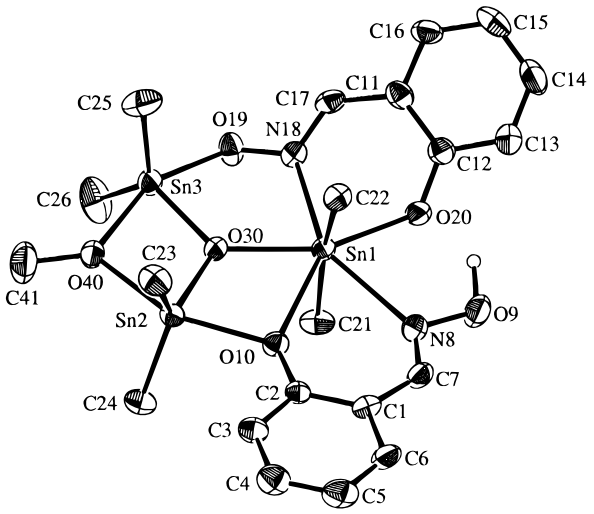

Figure 2. Molecular structure and crystallographic numbering scheme for [$(Me_2Sn)(Me_2SnO)(Me_2SnOMe)$(HONZO)-(ONZO)] (**3**); an analogous numbering scheme exists for compounds **4**−**6**.

3−**6** differ from the *a priori* expected compound **2a** by the fact that the two five-coordinate dimethyltin moieties are now bridged by a trifurcated oxygen atom of respectively a methoxy, ethoxy, *n*-propoxy, and isopropoxy group, rather than of a hydroxy group. For the remaining, the basic cluster core of the complexes remains the same, including the seven-coordinate tin atom.

When a mixture of dimethyltin(IV) oxide and salicylaldoxime in the molar ratio 1:1 is refluxed in benzene for a few hours, quick evaporation of the solvent gives rise to a crude, waxy solid, compound **2b**, which is, however, reasonably pure, as assessed by its melting point, elemental analysis, and NMR but which is unsuitable for X-ray diffraction analysis. Attempts to recrystallize **2b** in cyclohexane, *n*-hexane, or acetonitrile failed, the compound separating off as an oil upon cooling of the solvent. Crystallization was successful in methanol, ethanol, 1-propanol, or 2-propanol but failed to generate crystals of compound **2b**, compounds **3**−**6** being respectively generated instead. Accordingly, compound **2b** was characterized in solution only, mainly by NMR. Details on the synthesis and basic characterization of all compounds, together with Mössbauer data, which conform to the presence of one seven-coordinate and two five-coordinate tin atoms, as observed previously,[2] are given in the Experimental Section.

X-ray Diffraction Analysis of Compounds 3−6. The molecular structure of the [$(Me_2Sn)(Me_2SnO)(Me_2$-SnOT)(HONZO)(ONZO)] compounds (T = Me (**3**), Et (**4**), *n*-Pr (**5**), *i*-Pr (**6**)) is exemplified in Figure 2 for **3**; selected interatomic parameters for all compounds are collected in Table 1.

The four structures are very similar to each other and are related closely to the structure of the hydroxy-bridged compound **1a**, [$(Bu_2Sn)(Bu_2SnO)(Bu_2SnO$**H**)-(HONZO)(ONZO)]; compounds **4**−**6** are isomorphous (Table 4). Clearly, the nature of the alkoxide (hydroxide) bridge between the Sn(2) and Sn(3) atoms does not exert a great influence on the overall structural motif. Given the similarity of the four structures, only a description of **3** will be given with specific details for

(4) (a) Keeler, J.; Clowes, R. T.; Davis, A. L.; Laue, E. D. *Methods Enzymol.* **1994**, *239*, 145. (b) Tyburn, J.-M.; Bereton, I. M.; Doddrell, D. M. *J. Magn. Reson.* **1992**, *97*, 305. (c) Ruiz-Cabello, J.; Vuister, G. W.; Moonen, C. T. W.; Van Gelderen, P.; Cohen, J. S.; Van Zijl, P. C. M. *J. Magn. Reson.* **1992**, *100*, 282. (d) Vuister, G. W.; Boelens, R.; Kaptein, R.; Hurd, R. E.; John, B. K.; Van Zijl, P. C. M. *J. Am. Chem. Soc.* **1991**, *113*, 9688.

Table 1. Selected Interatomic Parameters (Distances in Å and Angles in deg) for Compounds 3−6

	compd					compd			
	3	**4**	**5**	**6**		**3**	**4**	**5**	**6**
Sn(1)−O(10)	2.661(5)	2.678(5)	2.681(5)	2.647(8)	Sn(3)−O(19)	2.108(5)	2.089(5)	2.107(6)	2.111(9)
Sn(1)−O(20)	2.189(5)	2.198(5)	2.174(6)	2.192(8)	Sn(3)−O(30)	2.023(5)	2.033(4)	2.025(5)	2.039(7)
Sn(1)−O(30)	2.170(5)	2.175(4)	2.173(5)	2.170(7)	Sn(3)−O(40)	2.169(5)	2.150(5)	2.151(5)	2.195(8)
Sn(1)−N(8)	2.588(7)	2.603(6)	2.593(7)	2.60(1)	Sn(3)−C(25)	2.09(1)	2.108(9)	2.085(9)	2.10(1)
Sn(1)−N(18)	2.313(6)	2.307(6)	2.286(7)	2.33(1)	Sn(3)−C(26)	2.109(9)	2.104(9)	2.08(1)	2.10(1)
Sn(1)−C(21)	2.094(8)	2.099(7)	2.095(9)	2.10(1)	O(9)−N(8)	1.406(8)	1.416(7)	1.399(8)	1.42(1)
Sn(1)−C(22)	2.101(8)	2.103(7)	2.087(8)	2.11(1)	O(10)−C(2)	1.335(8)	1.350(8)	1.357(8)	1.36(1)
Sn(2)−O(10)	2.158(5)	2.151(5)	2.150(5)	2.146(7)	O(19)−N(18)	1.376(7)	1.371(7)	1.335(8)	1.34(1)
Sn(2)−O(30)	1.993(5)	2.018(4)	2.014(5)	1.996(7)	O(20)−C(12)	1.334(9)	1.335(8)	1.333(9)	1.30(1)
Sn(2)−O(40)	2.178(5)	2.156(5)	2.150(5)	2.141(8)	O(40)−C(41)	1.39(1)	1.408(9)	1.43(1)	1.36(2)
Sn(2)−C(23)	2.122(8)	2.093(8)	2.090(8)	2.10(1)	N(8)−C(7)	1.272(9)	1.261(9)	1.27(1)	1.28(1)
Sn(2)−C(24)	2.103(8)	2.112(7)	2.090(9)	2.12(1)	N(18)−C(17)	1.280(9)	1.300(8)	1.35(1)	1.30(1)
O(10)−Sn(1)−O(20)	140.9(2)	138.6(2)	138.6(2)	138.9(3)	C(23)−Sn(2)−C(24)	131.8(3)	128.9(3)	128.7(4)	128.1(5)
O(10)−Sn(1)−O(30)	65.7(2)	65.3(1)	65.4(2)	65.0(2)	O(19)−Sn(3)−O(30)	85.2(2)	84.7(2)	85.3(2)	85.4(3)
O(10)−Sn(1)−N(8)	66.3(2)	65.9(2)	66.1(2)	66.5(3)	O(19)−Sn(3)−O(40)	155.6(2)	155.6(2)	158.3(2)	156.6(3)
O(10)−Sn(1)−N(18)	143.1(2)	143.4(2)	143.5(2)	144.3(3)	O(19)−Sn(3)−C(25)	100.1(3)	100.5(3)	90.2(3)	90.6(5)
O(10)−Sn(1)−C(21)	84.9(2)	84.4(2)	86.9(2)	85.1(4)	O(19)−Sn(3)−C(26)	89.3(3)	89.7(3)	96.3(3)	95.9(5)
O(10)−Sn(1)−C(22)	83.0(2)	86.1(2)	83.5(3)	84.9(4)	O(30)−Sn(3)−O(40)	73.1(2)	73.4(2)	73.5(2)	72.6(3)
O(20)−Sn(1)−O(30)	153.3(2)	155.9(2)	155.8(2)	155.6(3)	O(30)−Sn(3)−C(25)	107.8(3)	111.4(3)	123.3(3)	125.2(4)
O(20)−Sn(1)−N(8)	74.6(2)	72.7(2)	72.5(2)	72.7(3)	O(30)−Sn(3)−C(26)	122.9(4)	127.0(3)	115.2(3)	113.0(4)
O(20)−Sn(1)−N(18)	75.9(2)	78.0(2)	77.8(3)	76.7(3)	O(40)−Sn(3)−C(25)	97.0(3)	97.5(3)	97.5(3)	95.8(4)
O(20)−Sn(1)−C(21)	90.0(3)	94.0(3)	87.7(3)	86.7(4)	O(40)−Sn(3)−C(26)	93.3(3)	94.8(3)	96.8(3)	99.7(4)
O(20)−Sn(1)−C(22)	93.6(3)	86.4(3)	93.1(3)	95.0(4)	C(25)−Sn(3)−C(26)	129.0(4)	121.4(4)	121.5(4)	121.8(6)
O(30)−Sn(1)−N(8)	131.9(2)	131.2(2)	131.5(2)	131.4(3)	Sn(1)−O(10)−Sn(2)	95.7(2)	95.8(2)	95.5(2)	96.6(3)
O(30)−Sn(1)−N(18)	77.8(2)	78.4(2)	78.3(2)	79.5(3)	Sn(1)−O(10)−C(2)	139.6(4)	139.7(4)	139.9(5)	139.9(8)
O(30)−Sn(1)−C(21)	90.4(3)	92.4(2)	92.3(3)	92.3(4)	Sn(2)−O(10)−C(2)	124.4(4)	122.7(4)	122.1(5)	122.6(8)
O(30)−Sn(1)−C(22)	92.9(3)	92.8(2)	92.7(3)	91.6(4)	Sn(3)−O(19)−N(18)	117.1(4)	123.4(4)	122.7(5)	125.0(7)
N(8)−Sn(1)−N(18)	150.3(2)	150.2(2)	150.2(3)	148.9(4)	Sn(1)−O(20)−C(12)	124.4(5)	130.1(5)	130.5(5)	129.1(8)
N(8)−Sn(1)−C(21)	83.0(3)	83.4(2)	82.6(3)	83.6(4)	Sn(1)−O(30)−Sn(2)	119.1(2)	118.3(2)	118.2(2)	119.1(3)
N(8)−Sn(1)−C(22)	83.9(3)	83.5(3)	84.5(3)	84.2(4)	Sn(1)−O(30)−Sn(3)	127.9(2)	125.4(2)	125.4(2)	125.6(3)
N(18)−Sn(1)−C(21)	101.2(3)	93.4(3)	98.4(3)	100.0(4)	Sn(2)−O(30)−Sn(3)	112.7(2)	109.8(2)	110.2(2)	110.8(3)
N(18)−Sn(1)−C(22)	94.0(3)	100.2(3)	95.2(3)	93.4(4)	Sn(2)−O(40)−Sn(3)	100.5(2)	100.7(2)	100.7(2)	99.9(3)
C(21)−Sn(1)−C(22)	164.9(3)	166.2(3)	166.2(3)	166.6(5)	Sn(2)−O(40)−C(41)	130.3(6)	130.0(5)	123.7(5)	130(1)
O(10)−Sn(2)−O(30)	79.4(2)	78.9(2)	79.2(2)	78.3(3)	Sn(3)−O(40)−C(41)	128.8(5)	126.6(5)	127.7(5)	129(1)
O(10)−Sn(2)−O(40)	152.8(2)	152.4(2)	152.8(2)	152.9(3)	Sn(1)−N(8)−O(9)	109.3(4)	109.4(4)	109.8(5)	108.7(7)
O(10)−Sn(2)−C(23)	99.2(3)	95.5(3)	99.4(3)	98.2(4)	Sn(1)−N(8)−C(7)	139.1(6)	139.3(6)	139.5(6)	137(1)
O(10)−Sn(2)−C(24)	96.6(3)	99.3(3)	94.7(3)	95.2(4)	O(9)−N(8)−C(7)	111.6(7)	111.4(7)	110.5(7)	114(1)
O(30)−Sn(2)−O(40)	73.4(2)	73.6(2)	73.7(2)	74.6(3)	Sn(1)−N(18)−O(19)	120.1(4)	121.6(4)	123.0(6)	120.4(8)
O(30)−Sn(2)−C(23)	114.8(3)	114.3(3)	115.0(3)	116.8(4)	Sn(1)−N(18)−C(17)	124.8(6)	126.3(5)	125.1(7)	124.7(9)
O(30)−Sn(2)−C(24)	112.8(3)	116.5(2)	116.1(3)	114.9(4)	O(19)−N(18)−C(17)	114.8(6)	111.2(6)	111.6(7)	114(1)
O(40)−Sn(2)−C(23)	93.1(3)	94.1(3)	94.6(3)	94.9(4)	N(8)−C(7)−C(1)	127.2(7)	128.6(8)	127.0(8)	129(1)
O(40)−Sn(2)−C(24)	93.1(3)	94.5(3)	94.5(3)	95.2(4)	N(18)−C(17)−C(11)	126.6(7)	127.2(7)	127.7(9)	129(1)
O(9)/N(8)/C(7)/C(1)	−178.6(8)	−179.9(7)	176.7(8)	178(1)	O(19)/N(18)/C(17)/C(11)	−174.4(8)	176.7(7)	−175.6(8)	−179(1)
N(8)/C(7)/C(1)/C(2)	4(1)	3(1)	1(2)	−3(2)	N(18)/C(17)/C(11)/C(12)	19(1)	−10(1)	15(1)	16(2)
O(10)/C(2)/C(1)/C(7)	−4(1)	0(1)	1(1)	0(2)	O(20)/C(12)/C(11)/C(17)	−2(1)	4(1)	−6(1)	−6(2)

4−**6** following in parentheses. The structure is trinuclear with two distinct Sn atom geometries. The Sn(1) atom exists in a distorted-pentagonal-bipyramidal geometry with the axial positions occupied by the methyl substituents which define a C(21)−Sn(1)−C(22) angle of 164.9(3)° (166.2(3), 166.2(3), and 166.6(5)°). The pentagonal plane is defined by the O(10) and N(8) atoms of the uninegative HONZO ligand, the O(20) and N(18) atoms of the dinegative ONZO ligand, and the O(30) atom; the latter also bridges the Sn(2) and Sn(3) atoms and hence is tricoordinate. The five atoms defining the pentagonal plane are planar to ±0.068 Å (±0.044, ±0.065, and ±0.061 Å) and the Sn(1) atom lies 0.0043(5) Å (−0.0122(6), −0.0166(8), and 0.0046(5) Å) out of the plane in the direction of the C(21) atom. The Sn(2) and Sn(3) atoms are linked via the tricoordinate O(30) atom. A further link is provided by the O(40) atom of the alkoxide, which forms Sn−O bonds longer than those involving the O(30) atom; there are symmetrical bridges for **3**−**5**, but a difference of 0.05 Å in Sn−O is noted in the structure of **6**. The coordination of the $Me_2Sn(2)$ center is completed by the O(10) atom of the phenoxide group and that of $Me_2Sn(3)$ by the aldoximate O(19) atom. The Sn(2) and Sn(3) centers are thus five-coordinate and exist in distorted-trigonal-bipyramidal geometries. The Sn(2) atom lies 0.0690(5) Å (0.0613(6), 0.0420(8), and 0.0949(5) Å) out of the trigonal plane defined by the O(30), C(23), and C(24) atoms in the direction of the O(10) atom. Similarly, the Sn(3) atom lies 0.0511(5) Å (0.0209(6), 0.0208(9), and 0.0583(6) Å) out of the O(30)/C(25)/C(26) plane in the direction of the O(19) atom. Definitive evidence for the presence of O(9)*H* was found in **3**, as this atom was located in the X-ray analysis and a careful comparison of the geometric parameters in the remaining structures confirms protonation of the O(9) atoms; the O(9)H···O(20) separation is 1.66 Å. As indicated above, there is a HONZO anion as well as the ONZO dianion in each structure. Whereas the HONZO ion is essentially planar, there is a slight fold in the ONZO structure, as seen in the N(18)/C(17)/C(11)/C(12) torsion angles (Table 1). The closest non-H intermolecular contacts in the structure of **3** are C(1)···C(22) = 3.46(1) Å (symmetry operation $1 - x, -y, 1 - z$) and C(1)···C(24) = 3.46(1) Å (symmetry operation $1 - x, -y, 1 - z$); the closest contact involving the O(19) atom is 3.57(1) Å with C(25) (symmetry operation $1 + x, y, z$). In the structures of **4**−**6** the closest contacts of 3.40(1),

Table 2. ^{119}Sn, ^{13}C, and ^{1}H NMR Data from C_6D_6 Solutions of the Dimethyltin Moieties of Compounds 3−6, as Well as 2b[a]

compd	moiety	$\delta(^{119}Sn)$[b]	$^{n}J(^{119}Sn-^{119/117}Sn)$[c]	$\delta(^{13}C)$[d]	$^{1}J(^{13}C-^{119/117}Sn)$[e]	$\delta(^{1}H)$[f]	$^{2}J(^{1}H-^{119}Sn)$[g]
3	$Me_2Sn(1)$	−455.5	361,[h] 67[h]	14.8	1107/1058	1.08	114
	$Me_2Sn(2)$	−142.7	107,[h] 66[h]	1.6	671/641	0.44	76
	$Me_2Sn(3)$	−130.6	364/354, 108[h]	−1.1	659/629	0.42	76
4	$Me_2Sn(1)$	−457.2	350,[h] 66[h]	14.8	1110/1064	1.09	113
	$Me_2Sn(2)$	−144.3	108,[h] 67[h]	2.9	676/646	0.47	76
	$Me_2Sn(3)$	−132.8	360/345, 108[h]	0.1	660/634	0.45	76
5	$Me_2Sn(1)$	−457.9	355,[h] 68[h]	14.8	1106/1066	1.10	112[i]
	$Me_2Sn(2)$	−143.8	108,[h] 67[h]	2.8	678/646	0.49	74[i]
	$Me_2Sn(3)$	−132.5	360/345, 105[h]	0.0	659/629	0.47	74[i]
6	$Me_2Sn(1)$	−460.6	351,[h] 69[h]	14.9	1107/1061	1.10	114/109
	$Me_2Sn(2)$	−147.8	112,[h] 68[h]	5.1	679/647	0.54	75/72
	$Me_2Sn(3)$	−137.7	347,[h] 110[h]	1.9	668/638	0.51	75/72
2b	$Me_2Sn(1)$	−451.4	301,[h] 48[h]	14.9	1089/1047	1.10	113
	$Me_2Sn(2)$	−122.9	96,[h] 47[h]	3.1	648/622	0.59	74
	$Me_2Sn(3)$	−109.1	299,[h] 98[h]	0.8	642/616	0.57	75

[a] Chemical shift data in ppm and coupling constants in Hz. [b] ^{119}Sn resonances were referenced to the absolute frequency of Me_4Sn (37.290 665 MHz[18]); see Experimental Section. [c] Combined $^{3}J(^{119}Sn(1)-N(18)-O(19)^{119/117}Sn(3))$ and $^{2}J(^{119}Sn(1)-O(30)-^{119/117}Sn(3))$ coupling pathways, double $^{2}J(^{119}Sn(2)-O(30)-^{119/117}Sn(3))$ and $^{2}J(^{119}Sn(2)-O(40)-^{119/117}Sn(3))$ coupling pathways, and double $^{2}J(^{119}Sn(1)-O(30)-^{119/117}Sn(2))$ and $^{2}J(^{119}Sn(1)-O(10)-^{119/117}Sn(2))$ coupling pathways. [d] ^{13}C chemical shifts referenced to the solvent (C_6D_6) ^{13}C resonance and converted to the standard Me_4Si scale by adding 128.0 ppm. [e] Resolved $^{1}J(^{13}C-^{119}Sn)$ and $^{1}J(^{13}C-^{117}Sn)$ coupling satellites. [f] ^{1}H chemical shifts referenced to the residual solvent (C_6D_5H) ^{1}H resonance and converted to the standard Me_4Si scale by adding 7.15 ppm. [g] Pure $^{2}J(^{1}H-^{119}Sn)$ coupling constants determined from cross-sections along the F_2 axis (^{1}H nuclei) of 2D $^{1}H-^{119}Sn$ HMQC spectra at the ^{119}Sn resonance frequency along the F_1 axis of the corresponding tin atom, except for compounds **5** and **6** (see footnote *i*). [h] Averaged values from unresolved $^{n}J(^{119}Sn-^{119}Sn)$ and $^{n}J(^{119}Sn-^{117}Sn)$ coupling satellites in ^{119}Sn spectra. [i] Averaged values from unresolved $^{2}J(^{1}H-^{119}Sn)$ and $^{2}J(^{1}H-^{117}Sn)$ coupling satellites in standard ^{1}H spectra.

3.36(1), and 3.34(2) Å occur between the O(19) and C(16) atoms (symmetry operation x, $0.5 - y$, $0.5 + z$).

Close examination of the interatomic parameters of structures **3**−**6** shows that the substitution of the alkoxide group has no marked influence on the electronic structure of these systems. However, when the interatomic parameters of structures of **3**−**6** are compared with those of **1a**, [$(Bu_2Sn)(Bu_2SnO)(Bu_2SnO\mathbf{H})$-(HONZO)(ONZO)],[2] some bond distances associated with the Sn(1) atoms appear to be significantly different. Thus, the Sn(1)−O(20), Sn(1)−O(30), and Sn(1)−N(8) distances of 2.26(1), 2.14(1), and 2.67(1) Å appear to be longer, shorter, and longer, respectively, in **1a** than in **3**−**6**.

Solution-State Structures of Compounds 3−6. Basically, the ^{119}Sn NMR spectra as well as the ^{1}H spectra of C_6D_6 solutions in the ranges of the tin methyl and oximic protons are in agreement with the presence of three nonequivalent dimethyltin moieties, within which the methyl groups are isochronous, and two nonequivalent ligands, HONZO and ONZO. In general, minor resonances from species generated *in situ* upon dissolution are likewise observed, nevertheless to variable extents, depending on solution and/or solvent aging as well as on the nature of the compound. Among these transient solution species, the dimethyltin analog of the minor species m_2 observed in solutions of compound **1a**[2] provides a pair of equally intense ^{119}Sn resonances at −126 and −220 ppm (±1 ppm, because of a slight concentration dependence) for all compounds, reflecting an instability ranking for their group T in the order **3** < **4** ≈ **5** ≪ **6**. Analogously, the dimethyltin analog of species m_3[2] provides a single resonance at −282 ± 3 ppm, but its amount is much lower than in solutions of the dibutyltin compound **1a**. These observations indicate that the chemical mechanism previously discussed[2] to be responsible for the instability in solution of compound **1a** also holds for compounds **3**−**6**, with the alcohol TOH being eliminated rather than water. Further solution species are discussed below.

Table 2 presents an overview of the ^{119}Sn chemical shift data of compounds **3**−**6**, as well as the ^{1}H and ^{13}C chemical shift and coupling data for their dimethyltin moieties. The remaining ^{1}H and ^{13}C data are found in the Experimental Section.

The resonance assignment of compounds **3**−**6** has been achieved with roughly the same general assignment strategy[2] as for compound **1a**. Accordingly, we confine ourselves here to the main NMR characteristics of compounds **3**−**6**, relevant to their solution structures. The ^{119}Sn resonance around −455 ppm and the large magnitude of the associated $|^{1}J(^{13}C-^{119}Sn)|$ coupling constants[2,5] (>1000 Hz) are characteristic[2] for the seven-coordinate tin atom observed in the crystalline state of compounds **3**−**6** having a pentagonal-bipyramidal configuration with the two methyl groups in apical positions. In contrast, the two ^{119}Sn resonances between −130 and −140 ppm as well as the much lower $|^{1}J(^{13}C-^{119/117}Sn)|$ coupling constants on the order of 600−650 Hz,[2,5d] characterize the pair of five-coordinate tin atoms of compounds **3**−**6**. These coupling data are in agreement with the methyl groups occupying the equatorial positions of their trigonal-bipyramidal tin atoms. The presence of one dimethyltin ^{1}H resonance at higher frequency associated with a larger $|^{2}J(^{1}H-^{119/117}Sn)|$ coupling constant, as compared to the two other dimethyltin proton resonances, confirm the above structures.[6]

All four compounds exhibit a sharp OH(9) resonance around 13.8 ppm. This is in agreement with the hydroxylic proton H(9) being involved in a strong

(5) (a) Gielen, M.; Acheddad, M.; Bouâlam, M.; Biesemans, M.; Willem, R. *Bull. Soc. Chim. Belg.* **1991**, *100*, 743. (b) Gielen, M.; Acheddad, M.; Mahieu, B.; Willem, R. *Main Group Met. Chem.* **1991**, *14*, 73. (c) Gielen, M.; Bouâlam, M.; Biesemans, M.; Mahieu, B.; Willem, R. *Main Group Met. Chem.* **1991**, *14*, 271. (d) Holecek, J.; Lycka, A. *Inorg. Chim. Acta* **1986**, *118*, L15.

(6) Wrackmeyer, B. *Annu. Rep. NMR Spectrosc.* **1985**, *16*, 73.

intramolecular hydrogen bridge. While infrared data[7] in the solid state (ν_{OH} ~3480 cm^{-1}) confirm this hydrogen bridging to be essentially intermolecular, as observed also in the X-ray structures (see above), the IR data in CCl_4 (ν_{OH} ~3615−3655 cm^{-1}) support the proposal that this hydrogen bridge is intramolecular in solution (Figure 1).

As for compound **1a**,[2] tin specific assignment of the two high-frequency ^{119}Sn resonances around −140 and −130 ppm to the five-coordinate tin atoms Sn(2) and Sn(3) of **3**−**6** is not possible from the 1D spectra alone. In particular, the rather large $|^nJ(^{119}Sn-^{119/117}Sn)|$ coupling constant around 360 Hz does not establish unambiguously the uncommon $|^3J(^{119}Sn(1)-N(18)-O(19)-^{119/117}Sn(3))|$ coupling pathway rather than the more common $|^2J(^{119}Sn(1)-O-^{119/117}Sn(2))|$ one.[8]

In order to achieve a complete tin moiety and ligand specific assignment of all resonances of compounds **3**−**6**, we performed 2D $^1H-^{119}Sn$ HMQC[3d] correlation experiments.[2a,3c] In order to improve spectrum quality, and in particular to reduce artifacts, the 2D spectra were acquired with gradient pulse schemes,[4] to our knowledge for the first time for the ^{119}Sn nucleus (see Experimental Section). The 2D spectrum resulting from this type of experiment correlates proton $|^nJ(^1H-^1H)|$ multiplets in the F2 (detection) dimension with ^{119}Sn resonances in the F1 dimension. The correlation peaks arise exclusively from ^{119}Sn nuclei, which are coupled through a $|^nJ(^1H-^{119}Sn)|$ coupling pathway to the protons associated with these multiplets. This technique enables the observation of long-range $|^nJ(^1H-^{119}Sn)|$ couplings (n up to 5). The resulting coupling splittings can be determined to within typically 2 Hz, the usual digital resolution utilized for such 2D experiments. Smaller couplings remain detectable but appear as correlation cross peaks, the $|^nJ(^1H-^{119}Sn)|$ splitting of which is unresolved.

Figure 3 shows the cross-sections, parallel to the proton F2 axis, at each of the ^{119}Sn resonances along the F1 axis, as obtained from such a gradient-assisted 2D $^1H-^{119}Sn$ HMQC experiment for compound **3**. Table 3 summarizes all the $|^nJ(^1H-^{119}Sn)|$ correlation peaks observed for compounds **3** and **4**.

As for compound **1a**,[2] the ^{119}Sn resonance of the Sn(1) atom correlates with both the oximic protons H(7) and H(17) through $|^3J(^1H-^{119}Sn)|$ coupling pathways. The significant difference in coupling constant values is ascribed to the salicylaldoximate bonding network being planar for ligand A and distorted out of the cluster plane for ligand B, as found from the X-ray diffraction data.[2] In contrast, the ^{119}Sn resonances of the Sn(2) and Sn(3) atoms correlate with only the oximic proton H(17) through long-range $|^nJ(^1H-^{119}Sn)|$ coupling pathways (n = 5 for Sn(2), n = 4 for Sn(3)). This correlation pattern between the ^{119}Sn nuclei and the oximic protons is in agreement with the solid-state structure of these compounds. A correlation of the Sn(2) and Sn(3) atoms with the oximic proton H(7) is not detected, which is acceptable since it should arise from $|^5J(^1H-^{119}Sn)|$ coupling pathways involving long Sn−O bonds.

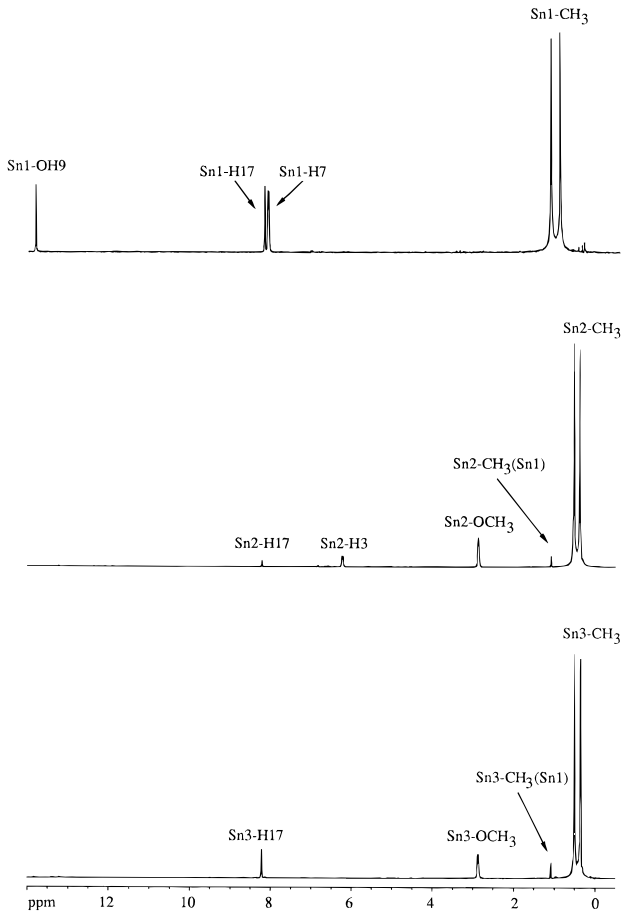

Figure 3. Cross-sections, parallel to the F_2 axis (proton resonances), of the gradient-assisted 2D $^1H-^{119}Sn$ HMQC spectrum of compound **3** at the ^{119}Sn resonance frequency along the F1 axis (^{119}Sn nuclei) of the Sn(1) (top), Sn(2) (middle), and Sn(3) (bottom) atoms. All cross-peaks are labeled in terms of the $^1H-^{119}Sn$ HMQC correlation pairs associated with tin nuclei and protons labeled according to the atom-labeling scheme of Figure 1.

The existence of the alkoxy group bridging the Sn(2) and Sn(3) atoms of compounds **3** and **4** in solution is unambiguously confirmed by the presence of two strong, equally intense $|^3J(^1H-^{119}Sn)|$ correlation peaks between the α−protons of the alkoxy group and the tin atoms Sn(2) and Sn(3). No correlation is observed with the tin atom Sn(1), being a $|^5J(^1H-^{119}Sn)|$ coupling pathway involving two additional rather long Sn−O bonds which appear to be poor long-range-coupling transmitters. On the other hand, a weak long-range $|^4J(^1H-^{119}Sn)|$ correlation is even observed between the ethoxy methyl group and both tin atoms Sn(2) and Sn(3) in compound **4**. The $|^3J(^1H-^{119}Sn)|$ correlation, which is only weak, between the hydroxylic proton OH-(9) and the tin atom Sn(1) is in agreement with the intramolecular hydrogen bond between the OH(9) proton and the oxygen atom O(20).

As for compound **1a**,[2] the key to the full ^1H, ^{13}C, and ^{119}Sn resonance assignment is the existence of a $|^nJ(^1H-^{119}Sn)|$ correlation between an aromatic proton resonance and the ^{119}Sn resonance around −140 ppm associated with a five-coordinate tin atom. The corre-

(7) Silverstein, R. M.; Bassler, C. G.; Morrill, T. C. *Spectrometric Identification of Organic Compounds*, 5th ed.; Wiley: New York, 1991; Chapter 3, pp 110−111, 158.

(8) (a) Gielen, M.; El Khloufi, A.; Biesemans, M.; Willem, R. *Appl. Organomet. Chem.* **1993**, *7*, 119. (b) Gielen, M.; Meunier-Piret, J.; Biesemans, M.; Willem, R.; El Khloufi, A. *Appl. Organomet. Chem.* **1992**, *6*, 59. (c) Yano, T.; Nakashima, K.; Otera, J.; Okawara, R. *Organometallics* **1985**, *4*, 1501. (d) Lockhart, T. P.; Manders, W. F.; Brinckman, F. E. *J. Organomet. Chem.* **1985**, *286*, 153. (e) Lockhart, T. P.; Puff, H.; Schuh, W.; Reuter, H.; Mitchell, T. N. *J. Organomet. Chem.* **1989**, *366*, 61. (f) Puff, H.; Schuh, W.; Sievers, R.; Wald, W.; Zimmer, R. *J. Organomet. Chem.* **1984**, *260*, 271.

Table 3. $^1H-^{119}Sn$ Correlation Data As Obtained from 2D $^1H-^{119}Sn$ HMQC Spectra Recorded from C_6D_6 Solutions of Compounds 3 and 4, as Well as 2b[a]

compd	tin atom	$\delta(^{119}Sn)$[b]	oximic protons[c]	other protons[c]
3	Sn(1)	−455.5	H(7): 8.12, $^3J = 12$ H(17): 8.21, $^3J = 4$	OH(9): 13.82, $^3J < 2$ H(3′): 7.03 (weak)
	Sn(2)	−142.7	H(7): − H(17): 8.21, $^5J < 2$	H(3): 6.22, $^4J = 14$ OCH_3: 2.86, $^3J = 11$ $CH_3-Sn(1)$: 1.08 (weak) H(5): 6.60 (weak) H(6): 6.83 (weak)
	Sn(3)	−130.6	H(7): − H(17): 8.21, $^4J = 4$	OCH_3: 2.86, $^3J = 13$ $CH_3-Sn(1)$: 1.08 (weak)
4	Sn(1)	−457.2	H(7): 8.13, $^3J = 12$ H(17): 8.21, $^3J = 4$	OH(9): 13.87, $^3J < 2$
	Sn(2)	−144.3	H(7): − H(17): 8.21, $^5J < 2$	H(3): 6.24, $^4J = 13$ OCH_2CH_3 CH_2: 3.14, $^3J = 12$ CH_3: 0.70, $^4J < 2$ $CH_3-Sn(1)$: 1.09 (weak)
	Sn(3)	−132.8	H(7): − H(17): 8.21, $^4J = 4$	OCH_2CH_3 CH_2: 3.14, $^3J = 13$ CH_3: 0.70, $^4J < 2$ $CH_3-Sn(1)$: 1.09 (weak)
2b	Sn(1)	−451.4	H(7): 8.12, $^3J = 12$ H(17): 8.17, $^3J < 2$ H(27): −	OH(9): 13.70, $^3J < 2$
	Sn(2)	−122.9	H(7): − H(17): 8.17, $^5J < 2$ H(27): 7.82, $^4J < 2$	H(3): 6.11, $^4J = 13$
	Sn(3)	−109.1	H(7): − H(17): 8.17, $^4J < 2$ H(27): 7.82, $^4J < 2$	

[a] For each ^{119}Sn tin nucleus, the ^1H proton resonances (see Figure 3 for proton labeling) which display a correlation peak with the corresponding ^{119}Sn resonance are given together with their chemical shift (ppm) and the coupling constant (Hz). The correlations between tin nuclei and their own tin methyl protons are omitted for clarity, since they all correlate; their coupling constants are given in Table 2. [b] Chemical shifts in ppm (see Table 2). [c] Coupling constant values are resolved up to *ca.* 2 Hz, the digital resolution of the HMQC experiments.

sponding ^1H resonance being a doublet in the standard 1D ^1H spectrum, this correlation can reasonably arise only from the H(3)/Sn(2) pair through the long-range $|^4J(^1H-^{119}Sn)|$ correlation involving the coupling pathway $^1H(3)-C(3)-C(2)-O(10)-^{119}Sn(2)$. That no $|^4J(^1H-^{119}Sn)|$ correlation peak is observed for the coupling pathway $^1H(3)-C(3)-C(2)-O(10)-^{119}Sn(1)$ is explained by the Sn(1)−O(10) bond being longer (>2.6 Å) than the Sn(2)−O(10) bond (<2.2 Å). This confirms the observability of long-range $|^nJ(^1H-^{119}Sn)|$ coupling pathways through Sn−O bonds to be sensitive to the Sn−O bond length.

Starting from the unambiguous H(3)/Sn(2) cross-peak, the $|^2J(^1H-^{119}Sn)|$ HMQC cross-peaks specifically associate the methyl tin ^1H resonances with the ^{119}Sn atoms of the dimethyltin moieties they belong to. Subsequently, the $|^1J(^1H-^{13}C)|$ cross-peaks from a 2D $^1H-^{13}C$ HMQC experiment[9] could be directly assigned to the associated methyl carbon atoms. Other minor but not unimportant $^1H-^{119}Sn$ HMQC cross-peaks that could not be observed previously[2] for **1a** in $^1H-^{119}Sn$ HMQC experiments without gradient pulses[4] become visible for compounds **3** and **4**. These cross-peaks correlating the ^{119}Sn nuclei of tin atoms Sn(2) and Sn(3) with the methyl protons of Sn(1), of the tin atom Sn(1) with the aromatic proton H(3′), and of the tin atom Sn(2) with the aromatic protons H(4), H(5), and H(6) support our final assignment.

On the other hand, aromatic ^{13}C chemical shift arguments[10a] and ^{13}C DEPT spectra[10] provided a preliminary rough, ligand-unspecific assignment of the aromatic ^{13}C resonances. When this rough assignment was combined with the specific ligand A assignment for proton H(3) outlined above, the specific ligand A and B assignments of the aromatic ^1H and ^{13}C resonances were completed from 2D $^1H-^{13}C$ HMQC−COSY[9] and 2D $^1H-^{13}C$ HMBC spectra (Experimental Section).[3a,b] The similarity between the ^1H, ^{13}C, and ^{119}Sn NMR data of compounds **3**−**6** is such that the ^1H and ^{13}C assignments for **5** and **6** (Table 2 and Experimental Section) were achieved without 2D NMR, by simple extrapolation from the data of **3** and **4**.

Solution-State Structure of Compound 2b. The final complete NMR assignments of compound **2b** are given in Table 2 and in the Experimental Section. The correlation data obtained from $^1H-^{119}Sn$ HMQC experiments are provided in Table 3. The structure proposed for compound **2b**, as deduced from all the NMR data, is given in Figure 4.

As for compounds **1a** and **1b**,[2] several common NMR 1D and 2D ^1H, ^{13}C, and ^{119}Sn features, especially the same basic $^1H-^{119}Sn$ HMQC cross-peak patterns, were obtained for the ligands A and B of compounds **2b**, **3**, and **4**. Thus, essentially the same cluster core, with the three tin atoms and the two ligands A and B, is present in **2b** as in **3**−**6**. The main difference resides in the presence of the third salicylaldoximate ligand C. The basic ^1H and ^{13}C resonance assignment of ligand C was

(9) Bax, A.; Griffey, R. H.; Hawkins, B. H. *J. Magn. Reson.* **1983**, *55*, 301.

(10) (a) Kalinowski, H. O.; Berger, S.; Braun, S. *Carbon-13 NMR Spectroscopy*; Wiley: Chichester, U.K., 1988. (b) Doddrell, D. M.; Pegg, D. T.; Bendall, M. R. *J. Magn. Reson.* **1982**, *48*, 323. (c) Bendall, M. R.; Doddrell, D. M.; Pegg, D. T. *J. Am. Chem. Soc.* **1981**, *103*, 4603. (d) Bendall, M. R.; Pegg, D. T. *J. Magn. Reson.* **1983**, *53*, 272.

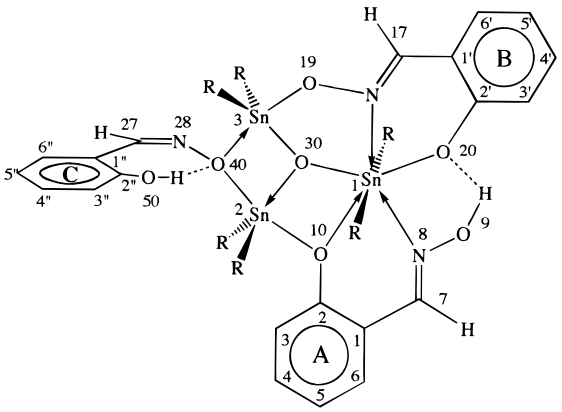

Figure 4. Structure, with atom labeling, in C_6D_6 solution, of the compound **2b** obtained after rapid solvent evaporation of the mixture resulting fom the condensation reaction between dimethyltin(IV) oxide and salicylaldoxime in the molar ratio 1:1.

achieved as for the ligands A and B of **2b**, **3,** and **4** from 2D $^1H-^{13}C$ HMQC−COSY[9] and 2D $^1H-^{13}C$ HMBC[3a,b] spectra.

The NMR features relevant to the structure elucidation of **2b** are as follows. The oximic proton H(27) of ligand C exhibits two equally intense $^1H-^{119}Sn$ HMQC cross-peaks with the tin atoms Sn(2) and Sn(3). As for compound **1b**,[2] this suggests that ligand C is involved in a bonding structure including the two oxygen-bridged five-coordinate tin atoms Sn(2) and Sn(3). This is reinforced by the absence of a cross-peak between the oximic proton H(27) and the seven-coordinate tin atom Sn(1). As such, compound **2b** can be seen formally as any of the alkoxy complexes **3**−**6** in which the bridging alkoxy group is substituted by a third, monoprotic salicylaldoximate residue, ligand C. These data are in agreement with a structure for **2b** that would simply be the dimethyltin analog of the structure[2] proposed for compound **1b**, involving the phenolic oxygen atom of ligand C as a bridging moiety between the tin atoms Sn(2) and Sn(3). Actually, this bond network for **1b** is incorrect, as revealed by the following data.

An additional, rather narrow OH singlet at 10.8 ppm indicates the presence of a second hydroxylic proton in compound **2b**. A rather broad IR band in CCl_4 solution at ν_{OH} 3586 cm^{-1} suggests that both hydroxylic protons are involved in weak intramolecular hydrogen bonding. The OH ^1H resonance at 10.8 ppm does not exhibit any $^1H-^{119}Sn$ HMQC cross-peak, unlike the OH(9) resonance at 13.8 ppm, which exhibits a cross-peak with the ^{119}Sn resonance of the Sn(1) tin atom, as do compounds **3** and **4**.

The 2D $^1H-^{13}C$ HMBC[3a,b] spectrum of **2b**, shown in Figure 5, reveals a $^1H-^{13}C$ HMBC correlation cross-peak between the OH(9) hydroxylic ^1H resonance at 13.8 ppm and the C(7) oximic ^{13}C resonance of ligand A at 150.0 ppm. In contrast, the additional OH resonance at 10.8 ppm exhibits an intense $^1H-^{13}C$ HMBC cross-peak with the ^{13}C resonance of the C(2″) carbon atom at 158.9 ppm, but not with that of the C(27) oximic ^{13}C resonance of ligand C at 156.5 ppm. Moreover, weaker correlation peaks with the overlapping C(1″)/C(3″) ^{13}C resonances at 117.2 and 117.3 ppm, respectively, are also observed. These data establish unambiguously the hydroxylic proton OH(50) of ligand C as being bonded to the phenolic rather than the oximic oxygen atom,

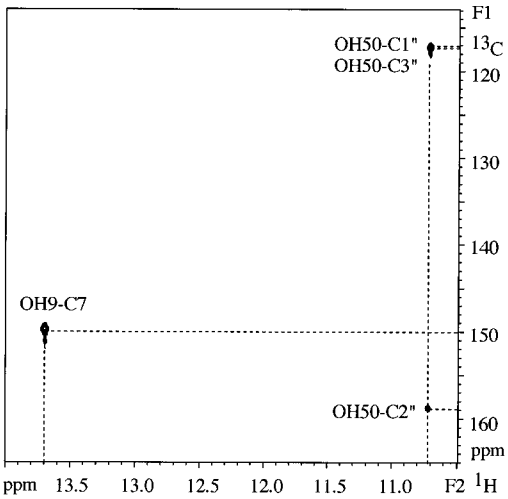

Figure 5. 2D $^1H-^{13}C$ HMBC spectrum of compound **2b** in the aromatic range for ^{13}C nuclei (F1, vertical axis) and in the hydroxylic proton range for ^1H nuclei (F2, horizontal axis). The cross-peaks between hydroxylic protons and carbon atoms are indicated. Those involving the OH(50) hydroxylic proton are relevant to the determination of the bonding mode of ligand C to the cluster structure of **2b**. Other spots correspond to spurious t_1 noise peaks.

unlike the case for ligand A. A ^{13}C SIMPLE-NMR experiment[2,11,12] confirmed this view, providing the secondary isotopic shift $\Delta = \delta(^{13}C-^2H) - \delta(^{13}C-^1H) = -0.233$ ppm upon deuterium substitution on the hydroxy groups at the C(2″) carbon atom and none at all at the C(27) atom. The two equally intense $^1H-^{119}Sn$ HMQC cross-peaks between the ^1H resonance H(27) and the ^{119}Sn resonances Sn(2) and Sn(3) reflect two $|^4J(^1H-^{119}Sn)|$ correlations through the $^1H(27)-C(27)-N(28)-O(40)-^{119}Sn(2)$ and $^1H(27)-C(27)-N(28)-O(40)-^{119}Sn(3)$ coupling pathways, respectively. Their equal intensities indicate that the two coupling pathways have similar geometries, which suggests the mean plane of the O(40)−N(28)−C(27)−C(1″)−C(2″)−O(50)−H(50)···O(40) seven-membered ring to be perpendicular or nearly so to the plane of the remaining cluster core. The bonding pattern proposed for ligand C is shown in Figure 4. Its stabilization by the weak hydrogen bond OH(50)···O(40) is uncertain, even if our IR data are in agreement with this proposal.

Resynthesizing the di-*n*-butyltin complex **1b**, according to the better method used here for compound **2b**, allowed us to record a 2D $^1H-^{13}C$ HMBC spectrum for **1b**. The similar correlation pattern obtained results in an analogous structure for **1b** as for **2b**.

Solution Chemistry. Compound **2b** is generated during the condensation reaction between salicylaldoxime and dimethyltin(IV) oxide as a noncrystallizable synthesis intermediate. The crystallization process in alcohols, by which crystals of compounds **3**−**6** are obtained from **2b,** is a reaction in which the alcohol acts as a nucleophile. An unusual nucleophilic substitution reaction substitutes the salicylaldoximate ligand C bridging the two five-coordinate tin atoms for a bridging alkoxy group. The hydroxylic proton of the entering

(11) (a) Christofides, J. C.; Davies, D. B.; Martin, J. A.; Rathbone, E. B. *J. Am. Chem. Soc.* **1986**, *108*, 5738. (b) Christofides, J. C.; Davies, D. B. *J. Am. Chem. Soc.* **1983**, *105*, 5099.

(12) Akitt, J. W.; Howarth, O. W. *J. Chem. Soc., Faraday Trans. 1* **1989**, *85*, 121.

alcohol converts the bridging ligand (HOZNO) into a good nucleophilic leaving group (HOZNOH), so that such substitutions are driven by proton transfer. Such reversible nucleophilic substitutions, which occur under mild room-temperature conditions at the Sn(2)−O−Sn(3) bridge, have been monitored by ^{119}Sn NMR studies *in situ*. The main results are as follows.

First, solutions in C_6D_6 of the alkoxy-bridged complexes are unstable, albeit only very slightly for **3**. Upon aging of the solution, the ^{119}Sn NMR spectra reveal the appearance in solution of **2a** and **2b** as transients, in addition to the above-mentioned dimethyltin analogs of m_2 and m_3. The hydroxy-bridged transient **2a** is characterized by its three ^{119}Sn resonances in the expected ranges, at −135, −147, and −458 ppm, and by the observation that addition of an excess (at least 10-fold) of water to a solution of either **3** or **2b** increases their intensities with respect to all other ^{119}Sn signals. Second, mixtures obtained at equilibrium after addition of a comparable excess of either water or free salicylaldoxime to a C_6D_6 solution of crystalline **3** reveal ^{119}Sn resonances from residual unreacted **3**. In contrast, addition of a similar excess of methanol, either to a solution of **2b** or to any equilibrated solution containing **2a**, **2b**, and **3** leads to a final solution containing **3** as the sole organotin compound. This matches the fact that the methoxy-bridged complex is isolated from methanol, rather than the hydroxy complex. Last, air equilibrated solutions of **2b** reveal the presence of 10% (maximum) of **2a**, indicating moisture sensitivity of **2b**. However, even in the presence of a 10-fold excess of water, residual **2b** remains visible. On the other hand, water added to pure **3** in solution generates not only **2a** but also **2b**. The conversion of **3** into **2b** without water occurs to a much lesser extent, meaning that the transient hydroxy complex **2a** itself provides the salicylaldoximate ligands necessary for the generation of the three-ligand complex **2b**.

This reversible conversion of **2a** and **2b** parallels that of the di-*n*-butyltin analogs **1a** and **1b**,[2] with, however, one major difference: while the hydroxy-bridged complex **1a** could be isolated in crystalline form, all attempts to isolate **2a** as such failed. In contrast, though the di-*n*-butyltin complexes **1a** and **1b** can substitute respectively water and salicylaldoxime for alcohols in solution, generation of crystals of the di-*n*-butyltin alkoxy analogs of **3**−**6** from alcohol solutions does not occur. Hence, in the presence of water, even only as traces in the alcohol or from the atmosphere, **1a** rather than di-*n*-butyltin alkoxy complexes is preferably generated, despite the larger amount of alcohol present.

Altogether, these data indicate that the nucleophilic substitution ability of the Sn(2)−O−Sn(3) functionality in the dimethyltin complexes decreases in the order Me−OH > HOZN−OH > H−OH. These results are summarized in Scheme 1, with single arrows indicating the thermodynamically favoured reaction sense.

At comparable molar excesses, ethanol substitutes the methoxy group of **3** (*ca.* 3% of residual **3** observed together with **4**) less efficiently than methanol substitutes the ethoxy group of **4** (no residual **4** observed).

Conclusion

The structure of complexes formed by the condensation of salicylaldoxime and diorganotin oxide in the molar ratio 2:3 displays a constant tin cluster core, with a seven-coordinate tin atom, two inequivalently bonded salicylaldoximate ligands, and a variable substituent on the trifurcated oxygen atom connecting two five-coordinate tin atoms, which depends on the nature of the diorganotin moiety. Crystalline material can be obtained for di-*n*-butyltin and dimethyltin salicylaldoximate complexes only when the two five-coordinate tin atoms are respectively hydroxy- and alkoxy-bridged. For both categories, the synthesis intermediate, which gives rise to these crystalline compounds, can be isolated but not crystallized as a 1:1 complex with three inequivalent salicylaldoximate ligands.

Scheme 1

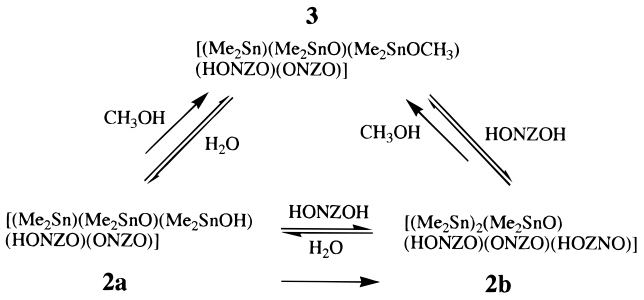

This investigation also demonstrates the major improvement in the quality of 2D ^{1}H−^{119}Sn HMQC spectra when appropriate magnetic field gradient pulses are inserted into the basic pulse sequence. Together with phase cycling, carefully adjusted gradients produce artifact−free spectra with no loss in signal sensitivity, at least for t_1 phase modulated spectra processed in the magnitude mode. Very weak proton−tin-119 correlations, relevant to the structure characterization of the compounds studied, are more reliably interpreted.

Experimental Section

Syntheses. A typical synthesis of compounds **3**−**6** was as follows. An amount on the order of 0.02 mol of salicylaldoxime was dissolved in 500 mL of either a mixture of toluene/ethanol (4/1 v/v) or benzene. Dimethyltin(IV) oxide was added in the ligand:oxide molar ratio 2:3. The reaction mixture was refluxed for 5 h with magnetic stirring. The ternary azeotrope ethanol/toluene/water, and subsequently, the binary azeotrope ethanol/toluene were distilled off with a Dean−Stark funnel, up to approximately 50% of the initial volume of the reaction mixture. The solvent was evaporated. Crystallization of the crude oily reaction mixture from methanol, ethanol, 1-propanol, or 2-propanol provided pure crystals of compounds **3**−**6**, respectively, suitable for X-ray analysis.

Compound **2b** was prepared by refluxing in benzene for 5 h a mixture of salicylaldoxime and dimethyltin(IV) oxide in the molar ratio 1:1. The azeotrope benzene/water was distilled off, the remaining solution filtered whenever necessary to remove small excesses of oxide, and the solvent eventually evaporated. A waxy, pale yellow solid was obtained. Attempts to crystallize **2b**, at room temperature after reflux or in the refrigerator, in *n*-hexane, cyclohexane, petroleum ether, acetonitrile, and chloroform failed, giving rise to an oil separating off from the solution. Crystallizations in methanol, ethanol, 1-propanol or 2-propanol provided crystals of **3**−**6**, respectively, as shown by melting point determinations and NMR spectroscopy. Attempts to further improve the purity of **2b** by column chromatography with silica gel and alumina or exclusion chromatography with Sephadex failed, giving rise to decomposition of the complex.

This synthetic method for compounds **3**−**6** via **2b**, even though 1 of the 3 equiv of salicylaldoxime involved was wasted,

Table 4. Crystallographic Data and Refinement Details for 3−6

	compd			
	3	**4**	**5**	**6**
formula	$C_{21}H_{32}N_2O_6Sn_3$	$C_{22}H_{34}N_2O_6Sn_3$	$C_{23}H_{36}N_2O_6Sn_3$	$C_{23}H_{36}N_2O_6Sn_3$
fw	764.6	778.6	792.6	792.6
cryst size, mm	0.13 × 0.16 × 0.32	0.13 × 0.19 × 0.37	0.08 × 0.29 × 0.40	0.07 × 0.24 × 0.32
cryst syst	monoclinic	orthorhombic	orthorhombic	orthorhombic
space group	$P2_1/c$	*Pbca*	*Pbca*	*Pbca*
a, Å	9.590(4)	20.078(3)	20.702(7)	21.367(2)
b, Å	23.30(1)	17.872(2)	17.783(5)	17.681(3)
c, Å	11.571(4)	15.267(3)	15.610(8)	15.327(2)
β, deg	103.53(3)			
V, Å^3	2729(1)	5478(1)	5746(6)	5790(1)
Z	4	8	8	8
D_{calcd}, g cm^{-3}	1.860	1.888	1.832	1.818
$F(000)$	1480	3024	3088	3088
μ, cm^{-1}	27.58	27.51	26.24	26.04
transmission factors	0.978−1.016	0.933−1.079	0.893−1.059	0.888−1.000
no. of data collcd	5334	6956	7291	7179
no. of unique data	4991	6956	7291	7179
no. of unique data with $I \geq 3.0\sigma(I)$	3161	3449	3338	2366
R	0.036	0.037	0.039	0.045
R_w	0.034	0.032	0.034	0.037
residual electron density, e Å^{-3}	0.49	0.66	0.48	0.54

usually led to easier crystallizations and slightly better overall yields and was therefore eventually the preferred one.

Dimethyltin(IV) oxide was prepared as previously described.[13]

Characterization. Mössbauer parameters in mm/s: IS = isomer shift, reference $Ca^{119}SnO_3$; QS = quadrupole splitting; Γ = line widths. IR data: ν_{OH} in cm^{-1}. NMR data: chemical shifts in ppm; coupling constants in Hz; for references, see the footnotes in Table 2; multiplicity patterns in ^{1}H spectra b = broad, d = doublet, dd = doublet of doublets, ddd = doublet of doublets of doublets, h = heptet, q = quartet, s = singlet, t = triplet, m = complex pattern, nr = nonresolved; $^nJ(^1H-^1H)$ coupling constants are given in brackets. ^{1}H chemical shifts, $^2J(^1H-^{119}Sn)$ coupling constants, ^{13}C chemical shifts, and $^1J(^{13}C-^{119/117}Sn)$ coupling constants for the tin methyl groups as well as the ^{119}Sn chemical shifts and $^nJ(^{119}Sn-^{119/117}Sn)$ coupling constants are given in Table 2 and are not repeated here.

Compound 3: yield 76%; mp 110−113 °C. Anal. Found: C, 32.61; H, 4.16; N, 3.65. Calcd for $C_{21}H_{32}O_6N_2Sn_3$: C, 32.98; H, 4.23; N, 3.66. Mössbauer: IS 1.06, 1.29; QS 2.60 (Γ 0.96/0.88), 4.08 (Γ 0.84/0.84). IR (CCl_4): ν_{OH} 3655 (w, sharp). IR (KBr): ν_{OH} 3494 (m, broad). ^{1}H NMR: H(3) 6.22, bd [8]; H(3′) 7.03, dd [7,2]; H(4), H(4′) 7.04−7.06, nr m; H(5) 6.60, dd [7,7]; H(5′) 6.55, ddd [8,6,2]; H(6) 6.83, dd [8,2]; H(6′) 6.80, dd [8,1]; H(7) 8.12, s; H(17) 8.21, s; OCH_3 2.86, s; OH(9) 13.82, s. ^{13}C NMR: C(1) 120.7; C(1′) 119.3; C2 161.0; C(2′) 162.6; C(3) 117.8; C(3′) 120.8; C(4) 131.0; C(4′) 132.4; C(5) 117.2; C(5′) 117.1; C(6) 135.5; C(6′) 132.1; C(7) 149.9; C(17) 154.7; OCH_3 48.7.

Compound 4: yield 75%; mp 115−118 °C. Anal. Found: C, 33.78; H, 4.39; Sn, 45.44. Calcd for $C_{22}H_{34}O_6N_2Sn_3$: C, 33.93; H, 4.41; Sn, 45.73. Mössbauer: IS 1.06, 1.29; QS 2.50 (Γ 0.83/0.78), 4.08 (Γ 0.75/0.75). IR (CCl_4): ν_{OH} 3615 (vw, sharp). IR (KBr): ν_{OH} 3210 (shoulder, broad). ^{1}H NMR: H(3) 6.24, d [8]; H(3′) 7.06, d [7], H(4), H(4′) 7.02−7.05, nr m; H(5) 6.60, dd [8,8]; H(5′) 6.56, dd [8,8]; H(6) 6.84, d [8]; H(6′) 6.81, d [8]; H(7) 8.13, s; H(17) 8.21, s; $OC\boldsymbol{H_2}CH_3$ 3.14, q [7]; $OCH_2C\boldsymbol{H_3}$ 0.77, t [7]; OH(9) 13.87, s. ^{13}C NMR: C(1) 120.6; C(1′) 119.3; C(2) 161.0; C(2′) 162.6; C(3) 117.8; C(3′) 120.8; C(4) 131.0; C(4′) 132.4; C(5) 117.2; C(5′) 117.1; C(6) 135.5; C(6′) 132.1; C(7) 149.9; C(17) 154.6; $O\boldsymbol{C}H_2CH_3$ 57.5; $OCH_2\boldsymbol{C}H_3$ 19.8.

Compound 5: yield 61%; mp 108−111 °C. Anal. Found: C, 34.69; H, 4.56; Sn, 44.75. Calcd for $C_{23}H_{36}O_6N_2Sn_3$: C, 34.85; H, 4.59; Sn, 44.92. Mössbauer: IS 1.03, 1.29; QS 2.50 (Γ 0.86/0.79), 4.06 (Γ 0.73/0.73). IR (CCl_4): ν_{OH} 3620 (vw, sharp). IR (KBr): ν_{OH} 3440 (w, broad). ^{1}H NMR: H(3) 6.24, d [8]; H(3′), H(4), H(4′) 7.03−7.10, nr m; H(5) 6.60, dd [7,7]; H(5′) 6.57, ddd [7,7,1]; H(6) 6.84, dd [8,1]; H(6′) 6.82, d [8]; H(7) 8.14, s; H(17) 8.22, s; $OC\boldsymbol{H_2}CH_2CH_3$ 3.08, t [7]; $OCH_2C\boldsymbol{H_2}$-CH_3 1.124, tq [7,7]; $OCH_2CH_2C\boldsymbol{H_3}$ 0.66, t [7], OH(9) 13.86, s. ^{13}C NMR: C(1) 120.7; C(1′) 119.4; C(2) 161.0; C(2′) 162.6; C(3) 117.9; C(3′) 120.9; C(4) 131.0; C(4′) 132.4; C(5) 117.2; C(5′) 117.1; C(6) 135.6; C(6′) 132.1; C(7) 149.9; C(17) 154.6; $O\boldsymbol{C}H_2$-CH_2CH_3 64.5; $OCH_2\boldsymbol{C}H_2CH_3$ 27.4; $OCH_2CH_2\boldsymbol{C}H_3$ 10.5.

Compound 6: yield 61%; mp 97−99 °C. Anal. Found: C, 35.25; H, 4.7; N, 3.6. Calcd for $C_{23}H_{36}O_6N_2Sn_3$: C, 34.85; H, 4.59; N, 3.53. Mössbauer: IS 1.03, 1.31; QS 2.52 (Γ 0.84/0.82), 4.08 (Γ 0.79/0.79). IR (CCl_4): ν_{OH} 3630 (vw, sharp). IR (KBr): ν_{OH} 3290 (m, broad). ^{1}H NMR: H(3) 6.25, d [8]; H(3′), H(4), H(4′) 7.03−7.07, nr m; H(5) 6.60, dd [8,8]; H(5′) 6.57, dd [8,8]; H(6) 6.85, dd [8,2]; H(6′) 6.82, dd [8,1]; H(7) 8.14, s; H(17) 8.21, s; $OC\boldsymbol{H}(CH_3)_2$ 3.51, h [6]; $OCH(C\boldsymbol{H_3})_2$ 0.76, d [6], OH(9) 13.90, s. ^{13}C NMR: C(1) 120.7; C(1′) 119.5; C(2) 161.1; C(2′) 162.6; C(3) 117.9; C(3′) 120.8; C(4) 130.9; C(4′) 132.3; C(5) 117.2; C(5′) 117.0; C(6) 135.5; C(6′) 132.0; C(7) 149.9; C17 154.4; $O\boldsymbol{C}H(CH_3)_2$ 65.1; $OCH(\boldsymbol{C}H_3)_2$ 26.9.

Compound 2b: yield 96%; mp 94−97 °C. Anal. Found: C, 36.96; H, 4.11; N, 4.71. Calcd for $C_{27}H_{35}O_7N_3Sn_3$: C, 37.28; H, 4.06; N, 4.83. Mössbauer: IS 1.40, 1.20, 0.60; QS 1.94 (Γ 0.85), 2.65 (Γ 0.83), 3.78 (Γ 0.94). IR (CCl_4): ν_{OH} 3586 (w, sharp). IR (KBr): ν_{OH} *ca.* 3200 (very weak, broad). ^{1}H NMR: H(3) 6.11, d [8]; H(3′) 7.05, nr; H(3″) 7.15, nr; H(4) 7.03, nr; H(4′) 7.09, nr; H(4″) 7.07, nr; H(5) 6.63, dd [7,7]; H(5′) 6.63, dd [7,7]; H(5″) 6.59, dd [7,7]; H(6) 6.85, d [7]; H(6′) 6.83, d [7]; H(6″) 6.86, d [7]; H(7) 8.12, s; H(17) 8.17, s; H(27) 7.82, s; OH(9) 13.78, s; OH(50) 10.80, s. ^{13}C NMR: C(1) 120.6; C(1′) 119.0; C(1″) 117.2; C(2) 160.2; C(2′) 162.4; C(2″) 158.9; C(3) 117.7; C(3′) 120.9; C(3″) 117.3; C(4) 131.3; C(4′) 132.8; C(4″) 131.2; C(5) 117.7; C(5′) 117.5; C(5″) 119.5; C(6) 135.6; C(6′) 132.2; C(6″) 130.3; C(7) 150.0; C(17) 155.5; C(27) 156.5.

Crystallography. Intensity data for the colorless crystals were measured at room temperature (20 °C) on a Rigaku AFC6R diffractometer equipped with graphite-monochromatized Mo Kα radiation (λ = 0.710 73 Å). The $\omega-2\theta$ scan technique was employed to measure data up to a maximum Bragg angle of 27.5°; the data sets were corrected for Lorentz and polarization effects,[14] and an empirical absorption correction was applied in each case.[15] Relevant crystal data are given in Table 4.

The structures were solved by direct methods employing SHELXS86,[16] and each was refined by a full-matrix least-

(13) Gielen, M.; Mancilla, T.; Ramharter, J.; Willem, R. *J. Organomet. Chem.* **1987**, *328*, 61.
(14) teXsan: Structure Analysis Software; Molecular Structure Corp., The Woodlands, TX.
(15) Walker, N.; Stuart, D. *Acta Crystallogr., Sect. A* **1983**, *39*, 158.

squares procedure based on F.[14] Non-H atoms were refined with anisotropic thermal parameters, and H atoms were included in the models in their calculated positions (C−H = 0.97 Å); the OH atom was located in the refinement of **3**. The refinements were continued until convergence, employing σ weights, and the analysis of variance showed no special features, indicating that an appropriate weighting scheme had been applied in each case. Final refinement details are collected in Table 4. Fractional atomic coordinates are available in the Supporting Information; the numbering scheme employed is shown in Figure 2 (drawn with ORTEP[17] at 35% probability ellipsoids). The teXsan[14] package, installed on an Iris Indigo workstation, was employed for all calculations.

NMR Experiments: Basics. The samples were prepared by dissolving ca. 40 mg of product in 0.5 mL of C_6D_6. Subsequently, most of the samples were degassed and sealed. All spectra were recorded at 303 K on a Bruker AMX500 spectrometer equipped with a digital lock and operating at 500.13, 125.77, and 186.50 MHz for ^{1}H, ^{13}C, and ^{119}Sn nuclei, respectively. Chemical shifts were referenced to the residual solvent peak (C_6D_6) and converted to the standard TMS scale by adding 7.15 and 128.0 ppm for ^{1}H and ^{13}C nuclei, respectively. The ^{119}Sn reference frequency was calculated from the absolute frequency of Me_4Sn, which is 37.290 665 MHz[18] at the B_0 field, corresponding to 100.000 000 MHz for the ^{1}H nuclei in TMS.

Broad-band ^{1}H-decoupled ^{13}C and ^{119}Sn spectra as well as ^{13}C DEPT spectra were recorded using the Bruker pulse sequences with standard delays. All heteronuclear correlation spectroscopy consisted of gradient-enhanced versions of the standard HMQC[9] and HMBC[3a,b] pulse sequences, all processed in the magnitude mode.

NMR Experiments: Gradient Assisted ^{1}H−^{119}Sn HMQC Spectroscopy. Historically, ^{1}H−^{13}C HMBC spectroscopy introduced the use of a low-pass filter[3a] in order to specifically edit multiple-bond ^{1}H−^{13}C correlations ($|^nJ(^1H-^{13}C)| \leq 20$ Hz) while suppressing the direct-bond ^{1}H−^{13}C correlations ($130 \leq |^1J(^1H-^{13}C)| \leq 160$ Hz) edited by ^{1}H−^{13}C HMQC spectroscopy.[3d] As a consequence of the large variety in $|^nJ(^1H-^{119}Sn)|$ coupling constant values and of the absence of $|^1J(^1H-^{119}Sn)|$ one-bond couplings in the structures of this work, the distinction between direct-bond and multiple-bond ^{1}H−^{119}Sn correlations becomes meaningless. Thus, though our experiments detect basically ^{1}H−^{119}Sn multiple-bond correlations, they were all obtained from a characteristic HMQC sequence[3d] without a low-pass filter. Accordingly, we adopt, throughout this paper, the nomenclature HMQC rather than HMBC when correlation experiments involving the ^{119}Sn nucleus are meant.

The benefits of gradient-determined coherence selection and/or artifact removal have been documented,[4a] especially for proton-detected ^{1}H−^{13}C and ^{1}H−^{15}N correlation experiments,[4b–d] but not, to the best of our knowledge, for proton-detected 2D ^{1}H−^{119}Sn HMQC[3] experiments.

Three sine-shaped B_0 gradients of 1 ms duration each were applied, prior to and immediately after the 180° ^{1}H pulse in the middle of the t_1 evolution period and after the last 90° X-nucleus pulse, respectively. Acquisition was started immediately after the last gradient pulse. The gradients were applied so as to selectively refocus the coherence pathway corresponding to heteronuclear double-quantum coherence prior to and heteronuclear zero-quantum coherence after the 180° ^{1}H pulse, and negative ^{1}H single-quantum coherence for detection. The associated refocusing condition for this pathway, $[(\gamma_H + \gamma_X)G_1 + (-\gamma_H + \gamma_X)G_2 - \gamma_H G_3] = 0$, has many solutions for the gradient strength ratio G_1:G_2:G_3.[4c] For the ^{1}H−^{13}C experiments gradient strengths were in a 5:3:4 ratio (G_1 = 12.5 T m^{-1}), which provides slightly better results in reducing artifacts than the more common 2:2:1 ratio (G_1 = 10.0 T m^{-1}).[19] All gradients were applied with a Bruker BGU−Z gradient unit, and pulse sequences were applied with the full standard phase cycle. 2D ^{1}H−^{13}C HMQC−COSY spectra were recorded with ^{13}C decoupling using GARP.[20] A total of 256 free induction decays (FID) of 4K data points, 8 scans each, were recorded covering a spectral width of 25 000 Hz in F1 and 7575 Hz in F2. The recycling delay was 2 s (including 0.27 s acquisition time). Data processing consisted of zero-filling to 1K in F1, followed by apodization with a squared sine bell with a shift of $\pi/2$ in both dimensions. The 2D ^{1}H−^{13}C HMBC spectra were optimized for average $|^{2,3}J(^{13}C-^1H)|$ values of 8.3 Hz (delay 60 ms). A low-pass J filter[3a,b] optimized to a $|^1J(^{13}C-^1H)|$ value of 135 Hz was used to suppress direct (HMQC-COSY like) correlations. The acquisition parameters were identical with those described above, except that 16 scans were averaged for each t_1 increment.

2D ^{1}H−^{119}Sn HMQC spectra were recorded with delays optimized for average $|^{2,3}J(^{119}Sn-^1H)|$ values between 8 and 4 Hz (delays ranging from 60 to 120 ms). As the ^{119}Sn resonances covered a very large spectral width, we preferred to record two spectra with a small ^{119}Sn window centered around the resonance areas from −100 to −150 ppm and −445 to −465 ppm, respectively. It was checked that back−folded cross-peaks in the F1 dimension did not interfere with the resonances of interest. A total of 64 or 32 FID's of 4K data points, 32 scans each, was recorded. Gradients were applied as described above except that the refocusing condition applied to the ^{119}Sn nucleus yields 50:45.65:40 for the gradient strength ratio (G_1 = 12.5 T m^{-1}).

For the ^{13}C and ^{119}Sn SIMPLE−NMR experiments,[11,12] partial deuteration corresponding to an HO:DO ratio of 60:40 was obtained by adding the appropriate amount of non-deuterated compound to a 0.5 mL C_6D_6 solution of fully deuterated **2b**. The latter was prepared by dissolving **2b** in CD_3OD, followed by evaporation under reduced pressure.

IR Data. Infrared data were acquired in the Fourier-transformed mode from a Perkin−Elmer System 200 FT−IR spectrometer.

Mössbauer Data. Mössbauer data were acquired and processed as previously described.[2a]

Acknowledgment. The financial support of the Belgian National Science Foundation (FKFO, Grant No. 2.0094.94) and of the Belgian "Nationale Loterij" (Grant No. 9.0006.93) is gratefully acknowledged (R.W., M.B.). Grants from the "Ministère des Affaires Culturelles du Luxembourg" (Grant BFR90/036) (F.K.), the "Comité National des Bourses OTAN" (F.K.), the "Ministère de l'Education Nationale du Luxembourg" (F.K.) and research grants from the Australian Research Council (E.R.T.T.) are gratefully acknowledged. We thank Mrs. I. Verbruggen for recording routine NMR spectra. We are indebted to the reviewers and the editor for valuable criticisms and suggestions.

Supporting Information Available: Further details of the structure determinations of **3**−**6**, including tables of atomic coordinates, bond distances and angles, and thermal parameters (28 pages). Ordering information is given on any current masthead page.

OM950928D

(16) Sheldrick, G. M. SHELXS86, Program for the Automatic Solution of Crystal Structure; University of Göttingen, Göttingen, Germany, 1986.

(17) Johnson, C. K. ORTEP; Report ORNL-5138; Oak Ridge National Laboratory, Oak Ridge, TN, 1976.

(18) (a) Mason, J. *Multinuclear NMR*; Plenum Press: New York, 1987; pp 625−629. (b) Davies, A. G.; Harrison, P. G.; Kennedy, J. D.; Puddephatt, R. J.; Mitchell, T. N.; McFarlane, W. *J. Chem. Soc. A* **1969**, 1136.

(19) Bermel, W. Report of Bruker Benelux User's Meeting, Antwerp, Belgium, 1992.

(20) (a) Barker, P. B.; Shaka, A. J.; Freeman, R. *J. Magn. Reson.* **1985**, *65*, 535. (b) Shaka, A. J.; Barker, P. B; Freeman, R. *J. Magn. Reson.* **1985**, *64*, 547.